 Bull. Chem. Soc. Jpn., 75, 2533–2539 (2002)

Self-Assembly of Amphoteric Azopyridine Carboxylic Acids II: Aspect Ratio Control of Anisotropic Self-Assembled Fibers By Tuning the π–π Stacking Interaction

Ken'ichi Aoki, Masaru Nakagawa, Takahiro Seki,* and Kunihiro Ichimura*,†

Chemical Resources Laboratory, Tokyo Institute of Technology, 4259 Nagatsuta, Midori-ku, Yokohama 226-8503

†Research Institute for Science and Technology, Science University of Tokyo, 2641 Yamazaki, Noda, Chiba 278-8510

(Received May 15, 2002)

Two ways to control the macroscopic morphology of fibrous organizates of amphoteric azopyridine carboxylic acids by tuning the strength of π–π stacking among the component molecules are presented. The self-organization of the azopyridine carboxylic acids (**1**–**5**) from aqueous solutions is governed not only by carboxyl/pyridyl hydrogen bondings, but also by dipole–dipole and π–π stacking interactions. The level of the latter could be tuned by the substituent structure at the phenyl ring. As a result, whereas leaflet crystals were formed from non-substituted derivative **1**, **3** with a propyl substituent gave fibrous assemblages, and needle-like assemblages were obtained from **2**, **4**, and **5** with methyl, *s*-butyl, and ethoxy substituents, respectively. The propyl-substitution is likely to enhance an anisotropic growth rate of the intermolecular hydrogen bonds due to efficient suppression of π–π stacking among aromatic cores, leading to the appearance of microfibers with the highest aspect ratio. The second way to control the organization morphology is based on "supramolecular copolymerization", which is attained by mixing **1** and **3** to modulate the strength of the π–π stacking. The aspect ratio of fibrous materials was significantly influenced by the mixing ratio.

Slight changes in the chemical structures of organic molecules sometimes result in significant differences in the macroscopic organization properties, which exhibit distinctive functionalities as consequences of molecular harmonization of the component molecules.[1] This situation is commonly observed in biological systems,[2] and also introducing simple substituent(s) to core moieties is known to make some types of medicines pharmacologically active. By mimicking such bio-related systems, one may be able to tailor supramolecular materials exhibiting specific macroscopic organization morphology and multiple properties through minimum efforts with trivial chemical modifications. The approaches to supramolecular structuring so far reported can be classified into the following categories. The first involves the chemical syntheses of a series of component molecules. Kunitake et al. discussed the relationship between the chemical structures and aggregation structures of single- and double-chain alkylammonium amphiphiles.[3] Shimizu et al. reported supramolecular assemblages formed from bolaform amphiphiles,[4a,b] the morphology of which is affected by the spacer length connecting both head groups. Closely related observations have been extensively made by several research groups.[5,6] The second method is to utilize external stimuli, such as heat and light. Kato et al.[7] and Griffin et al.[8] revealed that the organized structures of hydrogen-bonded supramolecular low-mass and polymeric liquid crystals are significantly affected by heat stimulus. Recently, light-responsive fibrous aggregates formed from cholesterol derivative tethered to the stilbene moiety were reported by Whitten et al.[9]

These two approaches have been widely utilized in studies on the self-assembly of supramolecular aggregates; to our knowledge, no systematic study has been achieved concerning a precise control of the shapes and growth direction of supramolecular aggregates in terms of the fine tuning of the chemical structures of component molecules and of the preparative conditions, except for the following examples. It was reported that the morphological features of organic microtubes and fibers (length distribution and thickness of wall) can be modulated by varying the preparation conditions, such as the solvent, concentration, cooling rate,[10] and cationic species in aqueous media,[4c] whereas the anisotropic growth of the fibrous materials has been achieved in a liquid-crystalline medium.[11]

In this context, we designed relatively simple molecules of amphoteric azopyridine carboxylic acids which display multiple non-covalent intermolecular interaction forces, including hydrogen bonds between carboxyl and pyridyl groups, π–π stackings among the aromatic rings, dipole–dipole and hydrophobic interactions (Fig. 1).[12a] It was found that self-organization behavior of the azopyridine carboxylic acids in an aqueous medium is critically affected by the structure of a side-substituent attached to the phenyl ring; the propyl substitution caused a reduction of the π–π stacking, resulting in changes in the organized morphology from leaflet crystals to well-defined microfibers with high aspect ratios.[12] This fact motivated us to tune the fibrous morphology, such as the diameter and length, by adequate side-chain substitution. Consequently, we investigated the self-organization of the azopyridine carboxylic acids with various side-substituents (**1**–**5**). We will also propose a

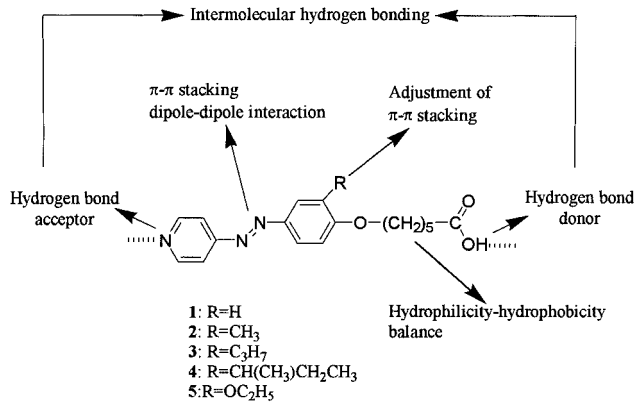

Fig. 1. Azopyridine carboxylic acids (**1**–**5**).

more convenient method for the morphology control by mixing two component molecules[5b] which show different levels of π–π stackings and dipole-dipole interactions.

Results

Effect of Side-Substituent on Self-Organization.

A. Self-Organization Behavior. Molecular assemblages of the azopyridine carboxylic acids (**1**–**5**) were prepared from alkaline aqueous solutions (10 mmol dm^{-3}) containing 3 molar amounts of NaOH. When the solutions were kept standing for several days under an atmospheric condition, the deposition of molecular assemblages occurred as the result of a gradual neutralization of the solutions by atmospheric carbon dioxide.[4b] Figure 2 shows optical micrographs of self-organized materials formed from the azopyridine carboxylic acids (**1**–**5**). All of the molecular assemblages formed from the side-substituted derivatives (Figs. 2b–e) exhibited characteristic microstructures with relative high aspect (length-to-diameter) ratios, while the non-substituted derivative (**1**) produced leaflet crystals, as shown in Fig. 2a. In particular, the self-organization of **3** bearing propyl-substituted gave well-defined fibrous assemblages having more than several hundred micrometers in length and 1

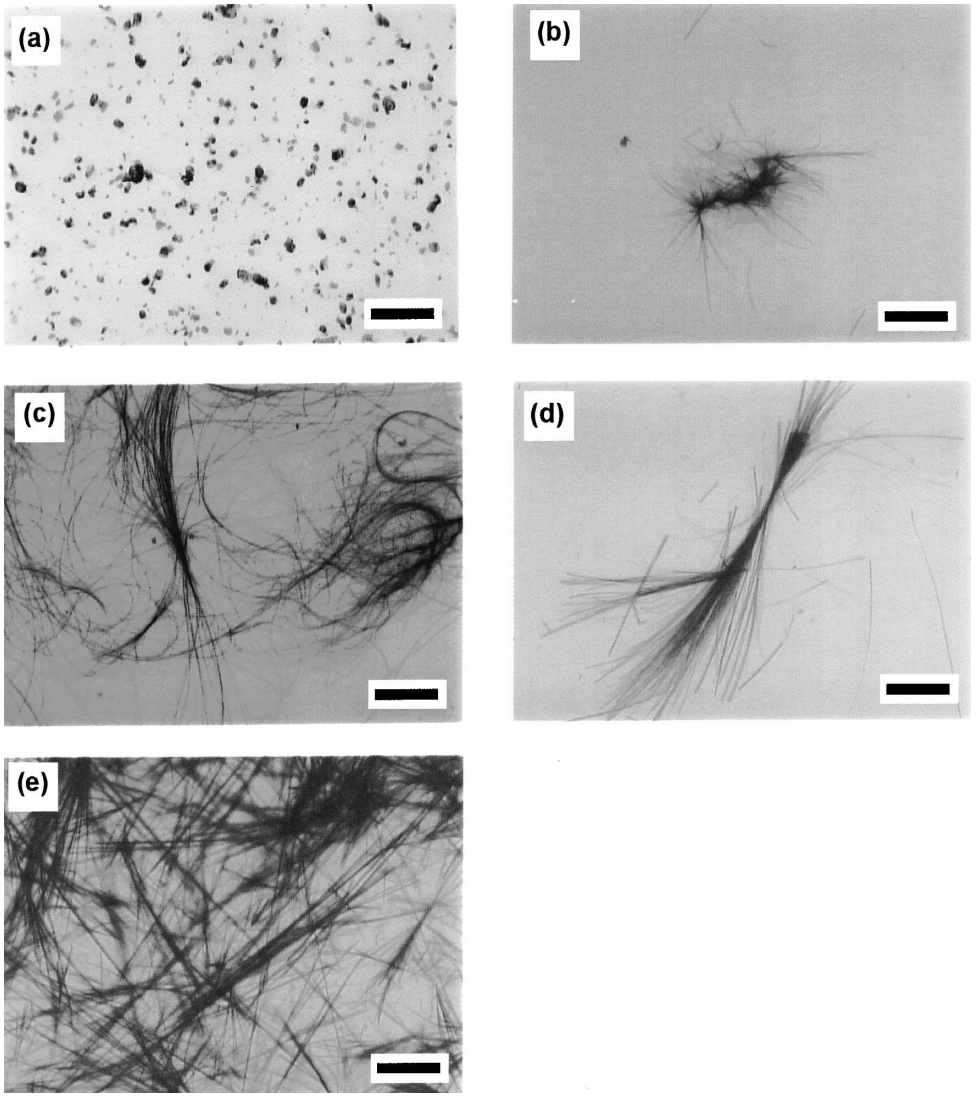

Fig. 2. Optical microscopes of molecular assemblages formed from (a) **1**, (b) **2**, (c) **3**, (d) **4**, and (e) **5** (scale bar: 200 μm).

μm in diameter. The aspect ratios of the self-assemblages derived from **2**–**5** were estimated to be ca. 30 for **2**, > 200 for **3**, ca. 50 for **4**, and ca. 30 for **5**. It is worth noting that the fibrous materials of **3** exhibit significantly high aspect ratios (> 200) compared with those of the other derivatives.

B. Powder X-ray Diffraction Analysis. Powder X-ray diffraction (XRD) measurements were carried out to investigate periodical molecular arrangements of self-organized materials. Figure 3 shows XRD diffraction patterns of molecular assemblages of **1**–**5** in a wet state. All of the XRD patterns of the self-assemblages formed from **2**–**5** are accompanied by a broad peak at $2\theta > 20°$, which is quite different from that of non-substituted **1**. These results indicate that the side-substitution at the aromatic core brings about a suppressive effect of the π–π stacking among the molecules, leading to an inhibition of crystallization.

C. FT-IR Analysis. The FT-IR spectra of the organized materials provide important information concerning the intermolecular hydrogen bonds among the component molecules. Figure 4 shows the FT-IR spectra of the molecular assemblages of **1**–**5** subjected to air-drying. All of the FT-IR spectra exhibited similar characteristic absorption bands of $\nu_{C=O}$, ν_{OH}, and the Fermi resonance band at around 1700, 2500, and 1930 cm^{-1}, respectively, indicating the formation of head-to-tail hydrogen bonds between carboxyl and pyridyl groups.[13] This provides evidence for the formation of supramolecular linear polymer structure, as shown in Fig. 1.

Self-Organization from Aqueous Solutions of Binary Mixtures. It seemed of great interest to investigate the self-organization from binary mixtures of **1** and **3** because these two compounds show the most different levels of the strength of the π–π stacking. Self-assemblages were prepared from alkaline solutions containing 3 molar amounts of NaOH in a total concentration of 10^{-2} mol dm^{-3}. The mixing ratio (R) was defined as $R = [\mathbf{3}]/([\mathbf{1}] + [\mathbf{3}])$, where [**1**] and [**3**] indicate the molar concentration of **1** and **3**, respectively.

A. Optical Microscopy Observation. Figure 5 shows optical micrographs of the resulting molecular assemblages formed from alkaline solutions of binary mixtures with various mixing ratios. In the region of $R > 0.4$, the morphologies of the materials altered from flexible fibers to rather shorter needle-like aggregates (Figs. 2c, 5a–c, and 2a) as the content of **1** was increased. In contrast, the self-assembly in the region of $R < 0.4$ gave more than two types of molecular assemblages, as can be seen in Figs. 5c and d.

B. DSC Analysis. Figure 6 shows DSC thermograms of each organized material on the first heating. DSC thermograms of the molecular assemblages formed from a single component of **1** and **3** were well consistent with those of pure compounds recrystallized from organic solvents, exhibiting endothermic peaks at 173 °C for **3** (Fig. 6a) and at 213 and 233 °C for **1** (Fig. 6e), respectively. On the other hand, DSC thermograms of the self-assemblages of $1.0 > R > 0.4$ exhibited an endothermic peak at 166–167 °C, as shown in Fig. 6b, and were quite different from those of pure **1** and **3**. These facts indicate that each molecule is incorporated into the organized systems in microscopic levels. In a region of $0.4 > R > 0$, DSC thermograms displayed a new broad peak at around 200–215 °C, and the transition enthalpy was enhanced as the content of **1** increased, as shown in Figs. 6c and d. This situation indicates the existence of more than two types of molecular assemblages in the region of $R < 0.4$.

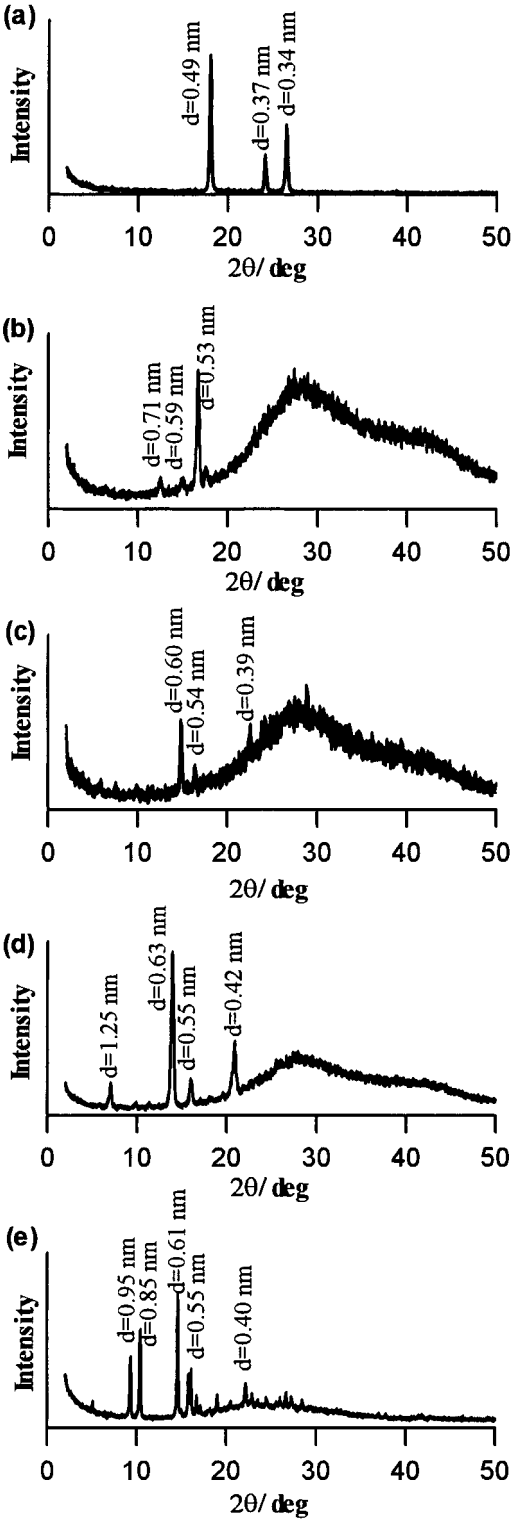

Fig. 3. Powder X-ray diffraction patterns of molecular assemblages of (a) **1**, (b) **2**, (c) **3** (d) **4**, and (e) **5** in a wet state.

C. XRD Analysis. XRD patterns of each molecular assemblage formed from binary mixtures of $1.0 > R > 0.4$ (Fig.

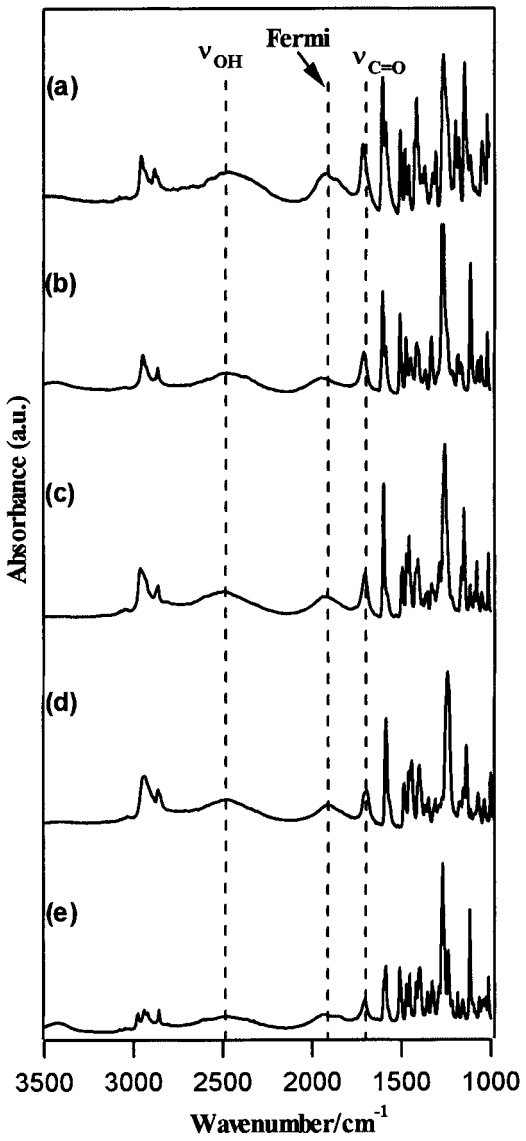

Fig. 4. FT-IR spectra of molecular assemblages of (a) **1**, (b) **2**, (c) **3**, (d) **4**, and (e) **5.**

7b) exhibited analogous diffraction peaks which are different from those of pure **3** and **1** (Figs. 7a and 7d). On the other hand, the XRD patterns of $0.4 > R > 0$ shown in Fig. 7c gave new diffraction peaks at $2\theta = 18.2°$, and 20.7° (d = 0.48, and 0.43 nm), indicating that a new organization structure appeared. These results are well consistent with the foregoing results derived from optical microscope and XRD measurements.

D. FT-IR Analysis. FT-IR spectra of the organized materials showed characteristic bands of $\nu_{C=O}$, ν_{OH} and the Fermi resonance at around 1700, 2500 and 1930 cm^{-1} (data not shown), indicating that the consecutive intermolecular hydrogen bonds between carboxyl and pyridyl groups are formed as described above. It is very likely that the head-to-tail hydrogen bonds lead to the formation of "supramolecular copolymers" of **1** and **3**.

E. ^{1}H NMR Spectra. The molar fractions of **3** in the molecular assemblages in $R > 0.4$ were estimated by the ^{1}H NMR spectra of dried organized materials dissolved in pyridine-d_5. The content of **3** was estimated from the integrated values of the peaks at 0.91 ppm due to the terminal CH_3 of the propyl residue. The molar fraction of **3** in the molecular assemblages was plotted as a function of the mixing ratio (R), as shown in Fig. 8. It was found that the molar fractions of **3** in the self-assemblages are in accordance with the initial mixing ratios of R in a region of $R > 0.4$.

Discussion

As shown in Fig. 1, hydrogen bonds contribute to the intermolecular forces parallel to the long axis of the component molecules, whereas π–π stacking and dipole-dipole interactions act as lateral forces, and the balance of these forces may play critical roles in determining the macroscopic organization morphology. In other words, as illustrated in Fig. 9, it is reasonably assumed that the suppressive effect of the lateral intermolecular interaction dominates the formation of the head-to-tail hydrogen bond between the pyridyl and carboxyl groups to give microfibers with a high aspect ratio.[12]

Our first strategy was to control the π–π stacking and the dipole-dipole interactions as the lateral intermolecular interaction forces by introducing a side substituent at the aromatic core. Compared with the non-substituted derivative of **1**, the side-substituted derivatives of **2**–**5** self-organized to give fibrous and/or needle-like non-crystalline assemblages with rather high aspect ratios (Figs. 2b–e), which may exhibit a broad peak at around $2\theta > 20°$ ($d < 0.44$ nm) in XRD patterns (Figs. 3b–e) due to the suppressive effect of the π–π stacking among the chromophores. The hydrogen bondings between the carboxyl and pyridyl groups in a head-to-tail manner, supported by FT-IR spectra shown in Fig. 4, are unlikely to be greatly influenced in their bond energies by the chemical structure because of minute electric contributions of the substituent at the phenyl ring to both of the basicity and acidity of pyridyl and carboxyl residues. Therefore, the aspect ratio of the self-assemblages is predominantly determined by the lateral non-covalent interaction forces. Propyl-substituted **3** exhibited the lowest melting point (172 °C) in a family of compounds (214–229 °C for **1**, 179–190 °C for **2**, 177 °C for **4**, and 185 °C for **5**). The propyl residue of **3** is larger in size than the hydrogen atom of **1** and the methyl of **2**, and possesses a larger degree of freedom compared with the *sec*-butyl of **4**. Moreover, compared with **5**, the absence of an ether linkage in the alkyl substitution of **3** causes much less induction of the dipole moment. Consequently, the lateral interaction forces are assumed to be minimized by introducing a propyl group. This situation is in accordance with the result that the fibrous assemblages of propyl substituted **3** exhibits the highest aspect ratio among all of the materials derived from the other compounds. This fact means that the macroscopic organization morphology of fibrous materials is controllable by adequate side-substitution at the aromatic core of the azopyridine carboxylic acids.

Since the modulation of the macroscopic morphology of fibrous materials by the effect of side-chain substitution requires a multi-step organic synthesis, we adopted an alternative strategy to control the organization morphology by mixing two kinds of component molecules. The combination of **1** and **3** was employed, while taking notice of their contrastive behav-

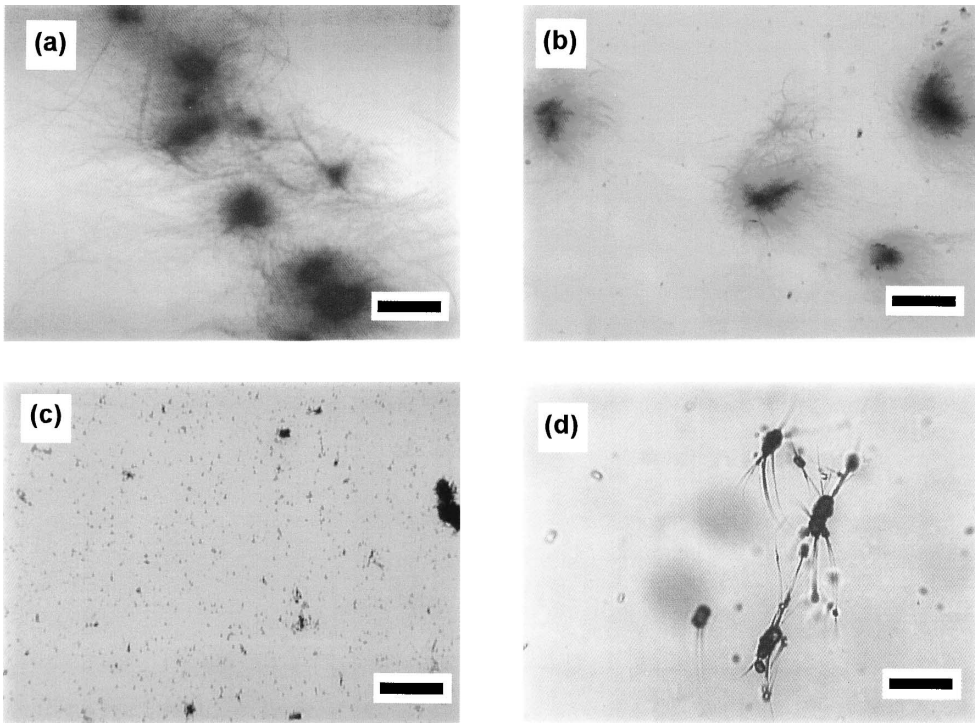

Fig. 5. Optical microscopes of molecular assemblages formed from binary mixtures of **1** and **3** in mixing ratios of R = (a) 0.7, (b) 0.5, (c) 0.3, and (d) 0.3 (under high magnification) (scale bar: 200 μm for a–c 20 μm for d).

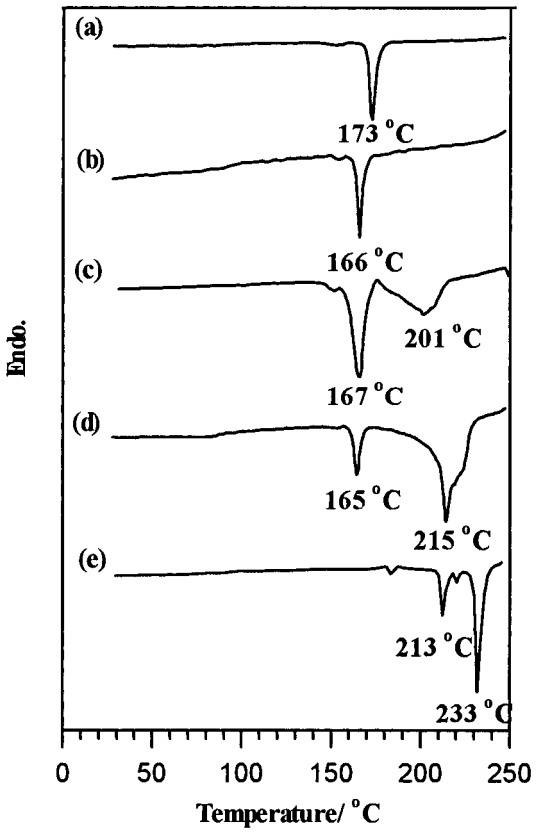

Fig. 6. DSC thermograms of molecular assemblages formed from binary mixtures of **1** and **3** in mixing ratios of R = (a) 1.0, (b) 0.5, (c) 0.37, (d) 0.2, and (e) 0.

ior in the self-organization. The self-organization of binary mixtures of **1** and **3** in the region of $R > 0.4$ gave hybridized molecular assemblages exhibiting a single endothermic peak at around 167 °C in DSC thermograms (Fig. 6b); their aspect ratios decreased with an increase in the fractions of **1**, as shown in Figs. 5a and b. On the other hand, in cases of $R < 0.4$, more than two kinds of molecular assemblages were formed, as shown in Figs. 5c and 5d, probably due to the strong π–π stackings to give a new broad peak at around 200–215 °C in DSC thermograms (Figs. 6c,d). These results are in line with the appearance of new diffraction peaks at 2θ =18.2° and 20.7° (d =0.49 and 0.43 nm), as observed in the XRD analysis shown in Fig. 7c. Furthermore, the compositions of **1** and **3** in each resulting molecular assemblage coincide well with the feeding mixing ratios (R) in the region of $R > 0.4$, as shown in Fig. 8. These results reasonably imply the formation of hydrogen-bonded "supramolecular copolymers" in which the copolymer ratios are determined by the feed ratios (R). Accordingly, non-covalent interaction forces in the lateral direction among the "supramolecular copolymers" was controlled conveniently and simply by mixing two component molecules to result in the manipulation of the aspect ratios of the novel fibrous materials.

Conclusion

It has been revealed that the precise morphology control of fibrous materials formed from alkaline aqueous solutions of azopyridine carboxylic acids is achievable in two ways by tuning the levels of both vertical and lateral non-covalent interaction forces among the rod-shaped molecules. The first ap-

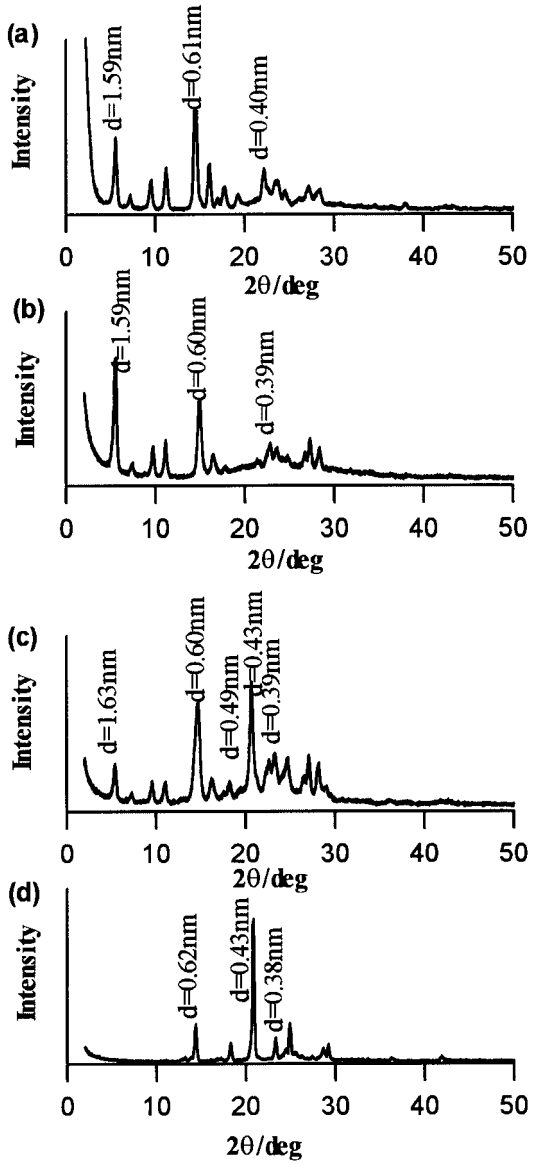

Fig. 7. Powder X-ray diffraction patterns of dried molecular assemblages formed from binary mixtures of **1** and **3** in mixing ratios of R = (a) 1.0, (b) 0.5, (c) 0.37, and (d) 0.

proach is based on a chemical modification of the side-substituent. Substitution with a propyl residue gives rise to the most effective suppression of the π–π stacking to enhance the consecutive anisotropic growth rate of intermolecular hydrogen bonds between the carboxyl and pyridyl groups in a head-tail manner, leading to the formation of microfibers with high aspect ratios. The second approach to modify the macroscopic morphologies of the assemblages involves the self-organization of binary mixtures of unsubstituted **1** and propyl-substituted **3** in an aqueous medium. The self-assemblages obtained from alkaline aqueous solutions containing $>$ 40% (mol/mol) of **3** provide "supramolecular copolymers" formed through the intermolecular head-to-tail hydrogen bonds. Since the compositions of **1** and **3** in the copolymers exactly reflect the feed ratios, the level of π–π stacking among the copolymers is likely to be reduced by the increased fraction of **1**, which results in a

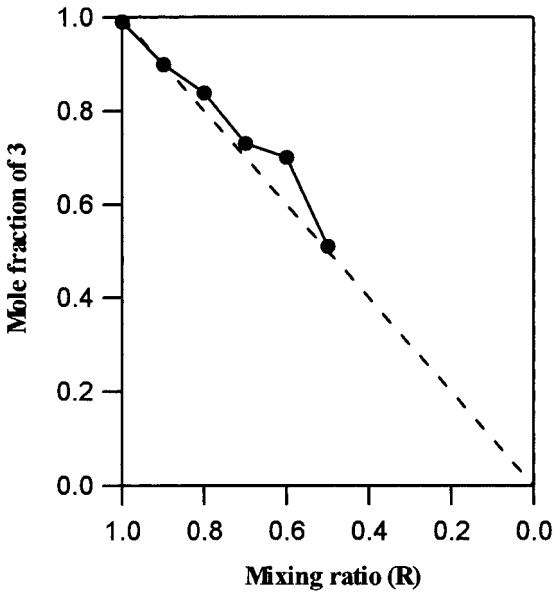

Fig. 8. Changes in mole fractions of **3** in molecular assemblages as a function of mixing ratio of R.

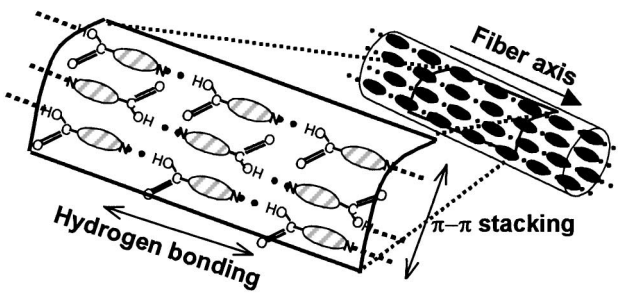

Fig. 9. Schematic representation of molecular assemblages formed from azopyridine carboxylic acids.

gradual decrease in the aspect ratio of the assemblages.

Experimental

Materials. All chemicals used here were of a reagent grade and were used without further purification. The synthesis of amphoteric azopyridine carboxylic acids (**1**–**5**) was reported elsewhere.[12b]

Physical Measurements. An optical microscopy observation of the morphology of organized materials was carried out using a BX-60 optical microscope (Olympus). ^{1}H NMR spectra were measured using an AC-200 NMR spectrometer (Bruker). FT-IR spectra were recorded on an FTS6000 spectrometer (Bio-Rad). Powder X-ray diffraction experiments were performed using a RINT2000 powder diffractometers (Rigaku). The Cu $K\alpha$ radiation of 1.54° was operated in a range of $2° < 2\theta < 50°$. DSC thermograms were taken on a DSC22C differential scanning calorimetry (Seiko Instruments) at a scanning speed of 5 °C min^{-1}. Phase-transition temperatures were adopted by reading the peak temperatures of DSC thermograms.

Deposition of Azopyridine Carboxylic Acids from an Alkaline Solution. Azopyridine carboxylic acids (**1**–**5**) were dissolved in a NaOH aqueous solution (3.0×10^{-2} mol dm^{-3}) to prepare transparent solutions at a concentration of 10^{-2} mol dm^{-3}.

The resultant solutions (2 mL) were placed in 5 mL vials, which were capped with an aluminum foil with small holes and kept standing for about two weeks under atmospheric conditions to allow spontaneous deposition. In binary systems of **1** and **3**, the mixing ratio (R) was defined as $R = [\mathbf{3}]/([\mathbf{1}] + [\mathbf{3}])$, where [**1**] and [**3**] indicate the molar concentration of **1** and **3**, and the total concentration is 10^{-2} mol dm^{-3}. In all cases including monomerous and binary systems, the self-organizations were examined under the same condition.

Sample Preparation for Physical Measurements. For optical microscope observations, each resulting molecular assemblage was put on a slide glass and capped with a cover glass. For XRD and FT-IR measurements, the molecular assemblages were isolated from water, washed with pure water three times, and dried under atmospheric conditions for several days. For ^{1}H NMR analysis, the isolated samples were dried in vacuo (100 °C) for 5 h and dissolved in pyridine-d_5 in a concentration of 0.3–0.5 wt%.

This works are financially supported by the Sasakawa Scientific Research Grant from the Japan Science Society (K. A.).

References

1 K. Ichimura, *Chem. Rev.*, **100**, 1847 (2000).

2 a) G. A. Jeffrey, "An Introduction to Hydrogen Bonding," Oxford University Press, New York (1997). b) G. A. Jeffrey and W. Saenger, "Hydrogen bonding in biological structures," Springer-Verlag, Berlin (1991).

3 a) T. Kunitake, Y. Okahata, M. Simomura, S. Yasunami, and K. Takarabe, *J. Am. Chem. Soc.*, **103**, 5401, (1981). b) M. Shimomura, R. Ando, and T. Kunitake, *Ber. Bunsen-Ges. Phys. Chem.*, **87**, 1134 (1983).

4 a) T. Shimizu and M. Masuda, *J. Am. Chem. Soc.*, **119**, 2812 (1997). b) T. Shimizu, M. Kogiso, and M. Masuda, *Nature*, **383**, 487 (1996). c) T. Shimizu, M. Mori, H. Minamikawa, and M. Hato, *J. Chem. Soc., Chem. Commun.*, **1990**, 183.

5 a) J.-H. Fuhrhop and W. Helfrich, *Chem. Rev.*, **93**, 1565 (1993). References are therein. b) J.-H. Fuhrhop, C. Boettcher, *J. Am. Chem. Soc.*, **112**, 1768 (1990).

6 a) J. S. Schneider, C. Messerschmidt, A. Schulz, M. Gnade, B. Schade, P. Luger, P. Bombicz, V. Hubert, and J. H. Fuhrhop, *Langmuir*, **16**, 8575 (2000). b) F. M. Menger, S. and J. Lee, *J. Am. Chem. Soc.*, **116**, 5987 (1994). c) T. Imae, L. Gagel, C. Tunich, G. Platz, T. Iwamoto, and K. Funayama, *Langmuir*, **14**, 2197 (2000).

7 a) T. Kato and J. M. J. Fréchet, *J. Am. Chem. Soc.*, **111**, 8533 (1989). b) T. Kato, J. M. J. Fréchet, P. G. Wilson, T. Saito, T. Uryu, A. Fujishima, and C. Jin, F. Kaneuchi, *Chem. Mater.*, **5**, 1094 (1993). c) T. Kato and J. M. J. Fréchet, *Macromol Symp.*, **98**, 311 (1995). d) H. Kihara, T. Kato, T. Uryu, and J. M. J. Fréchet, *Chem. Mater.*, **8**, 961 (1996). e) T. Kato, *Struct. Bond.*, **96**, 95 (2000).

8 a) C. Alexander, C. P. Jariwala, C.-M. Lee, and A. C. Griffin, *Macromol. Symp.*, **77**, 283 (1994). b) C.-M. Lee, C. P. Jariwala, and A. C. Griffin, *Polymer*, **35**, 4550 (1994). c) C.-M. Lee, and A. C. Griffin, *Macromol. Symp.*, **117**, 281 (1997).

9 C. Geiger, M. Stanescu, L. Chen, and D. G. Whitten, *Langmuir*, **15**, 2241 (1999).

10 a) B. N. Thomas, C. R. Safinya, R. J. Plano, and N. A. Clark, *Science*, **267**, 1635 (1995). b) M. S. Spector, J. V. Selinger, A. Singh, J. M. Rodrigues, R. R. Price, and J. M. Schnur, *Langmuir*, **14**, 3493 (1998). c) M. S. Spector, R. R. Price, and J. M. Schnur, *Adv. Mater.*, **11**, 337 (1999).

11 N. Mizoshita, T. Kutsuna, K. Hanabusa, and T. Kato, *Chem. Commun.*, **1999**, 781.

12 a) K. Aoki, M. Nakagawa, and K. Ichimura, *Chem. Lett.*, **1999**, 1205. b) K. Aoki, M. Nakagawa, and K. Ichimura, *J. Am. Chem. Soc.*, **122**, 10997 (2000).

13 S. L. Johnson and K. A. Rumon, *J. Phys. Chem.*, **69**, 74 (1965).